Estimation of Water Discharge from Gilgit Basin using Remote Sensing, GIS and Runoff Modeling

Furrukh Bashir[1], Dr. Ghulam Rasul[1]

Abstract

Northern Pakistan is one of the biggest repositories of snow and glaciated ice, outside polar region, throughout the world. Seasonal snow, bestowed by western depression on lofty mountains of HKH range in winter, generates runoff on melting in summers and, plays a significant role in shaping economy of Pakistan by providing hydrological resources for power generation and agriculture. Considering such vital significance of frozen water resources it is imperative to engineer a model to forecast potential availability of water from these frozen reserves. This strive is aimed to estimate runoff from Gilgit Basin in summer of 2003, by synergizing snow cover derived through remote sensing using Normalized Difference Snow Index (NDSI), digital elevation model and meteorological parameters in the snowmelt runoff model (SRM), eventually computed runoff is compared with measure runoff.

Keywords: Snowmelt Runoff Model, MODIS, NDSI, Gilgit Basin, Seasonal Melting, Snow Cover Monitoring.

Introduction:

Economy of Pakistan is largely dependent on hydrological resources for agriculture and power generation. A large portion of hydrological resources available to Pakistan is delivered by the melting of frozen reserves in Northern Pakistan in summers. These frozen reserves are comprised of seasonal snow cover and perennial glaciated ice. Scientific community is working hard to device a system that may forecast the potential availability of water from frozen hydrological reserves well-before melting time. Such forecast will be highly valuable for the planning in realm of hydroelectric power generation, flood control and hydro-resources management.

In literature, two main approaches are available to calculate snow melt and subsequent runoff; they are energy balance approach and temperature degree-day method. The energy exchange at snowpack surface can be explained by four major components as, the shortwave radiation exchange, long wave radiation exchange, convective heat transfer and advective heat transfer. These radiations exchanges and heat transfer can be estimated if information on various parameters as cloud covers, albedo, wind, cloud temperature and dew point temperature are known(Anderson, 1976). Information on these parameters is normally not available; therefore, degree-day approach is used for operational forecasting (Quick and Pipes, 1988). Degree-day approach has been successfully used to develop Snowmelt-Runoff Model (SRM). It is designed to forecast and simulate daily stream flow of mountainous basins (Rango and Martinec, 1995; Martinec, *et al*., 1994)

Northern Pakistan is one of the largest repositories of snow and glaciated ice outside Polar Regions. Runoff from mountainous glaciers and snowmelt is contributing significantly in overall stream runoff (Singh *et al*., 1997). Therefore, assessment of glacial and snow extent is important for estimation of stream runoff.

This endeavor is an attempt to calibrate Snowmelt Runoff Model (SRM) developed by Martinec (1975) for Gilgit basin. For this purpose melting season of year 2003 is chosen. Meteorological parameters like precipitation and temperature recorded by observatory of Pakistan Meteorological Department situated at Gilgit at 1460 m.a.s.l are used. Measured runoff gauged by Pakistan Water and Power Development Authority (WAPDA) at Alam Bridge Gilgit for 2003 is utilized.

[1] Pakistan Meteorological Department

Study Area:

A major part of the snow and glaciated ice of the Pakistan's HKH is concentrated in the watershed of the Indus basin. This watershed can be divided into ten distinct river basins, namely Indus, Jhelum, Shingo, Shyok, Shigar, Astor, Swat, Chitral, Gilgit and Hunza river. Out of these ten river basins Gilgit basin is selected as the study area. The river basin in the north is bordered with Afghanistan and China. The Gilgit River network comprises of the Ghizar, Yasin, Ishkuman and Hunza River and joins the Indus River near Jaglot. The upper reaches of the basin are mostly glaciated and covered with permanent snow.

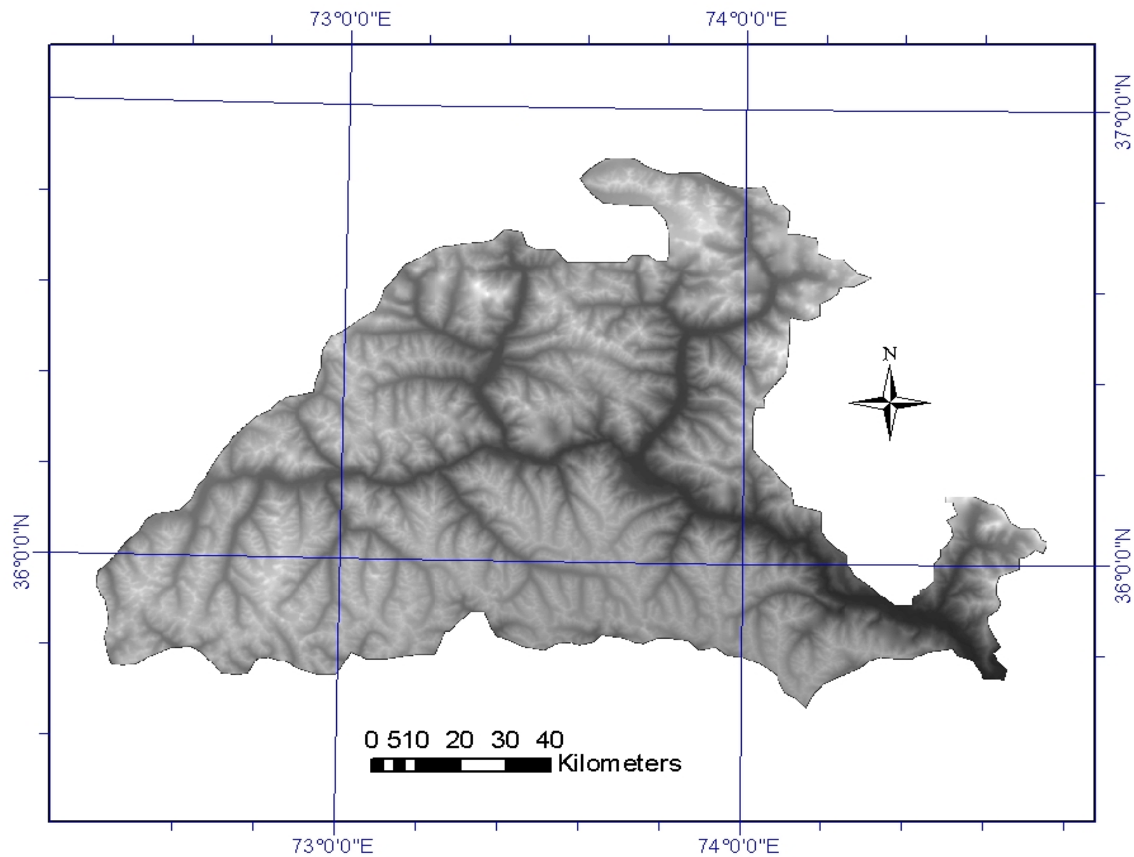

Figure 1: Gilgit Basin

Characteristics of Gilgit Basin:

The Gilgit basin boundary (Figure 1) is defined by the location of the streamgauge installed by WAPDA at Alam Bridge Gilgit, and the watershed divide is identified on a topographic map that is derived from Digital Elevation Model (DEM) made by Shuttle Radar Topography Mission (SRTM). After examining the elevation range between the streamgauge and the highest point in the basin (total basin relief), elevation zones are delineated in intervals of about 1000 m or 3280 ft as mentioned in Table 1.

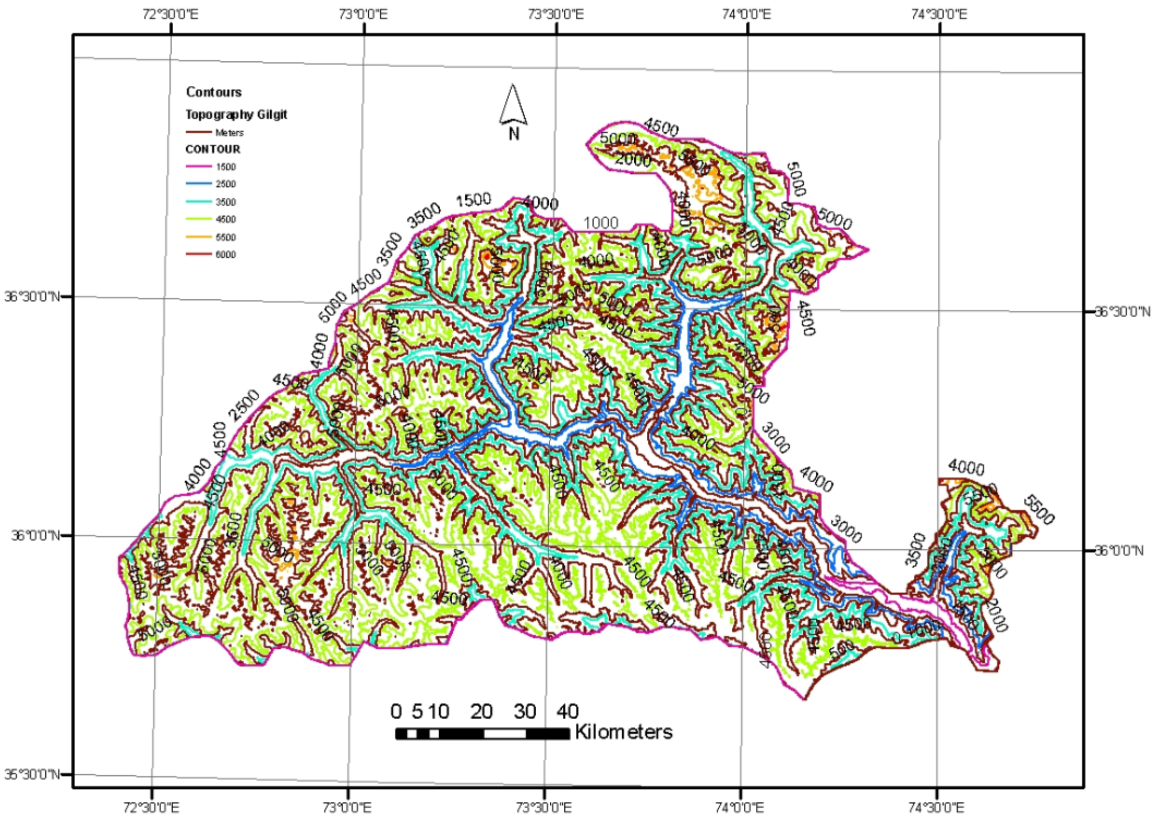

Figure 2: Topographic Map Gilgit Basin

Table 1: Division of Gilgit Basin According to Elevation Range and Area of Respective Zone

S.No	Zone Name	Elevation Range masl	Mean Hypsometric Height msal	Area (KM2)
1	A	1247-2500	2052	896
2	B	2500-3500	3091	2322
3	C	3500-4500	4083	6912
4	D	4500-5500	4782	3863
5	E	5500-6404	5660	311
Total				14304

(Figure2) shows contours delineation of zones in Gilgit Basin. Zone A ranges from 1274-2500 masl with mean hypsometric height at 2052 masl and area equals to 896 km^2. Zone B of Gilgit Basin ranges from 2500-3500 masl with mean hypsometric height as 3091masl and covers area of 2322km^2. Zone C covers spatial area of 6912km^2 i.e, largest zone with elevation range from 3500-4500 masl and mean hypsometric height as 4083 masl. Elevation ranges of Zone D is 4500-5500 masl with mean at 4782 masl and covers nearly 3863 km^2, second only to zone A. Last is zone E with least spatial coverage i.e, 311 km^2 only, and it ranges from 5500 to 6404 masl with mean at 5660 masl as expressed in Table 1. Snow cover is mapped on all elevation heights with the help of SRTM DEM as shown in Figure 2 and 3.

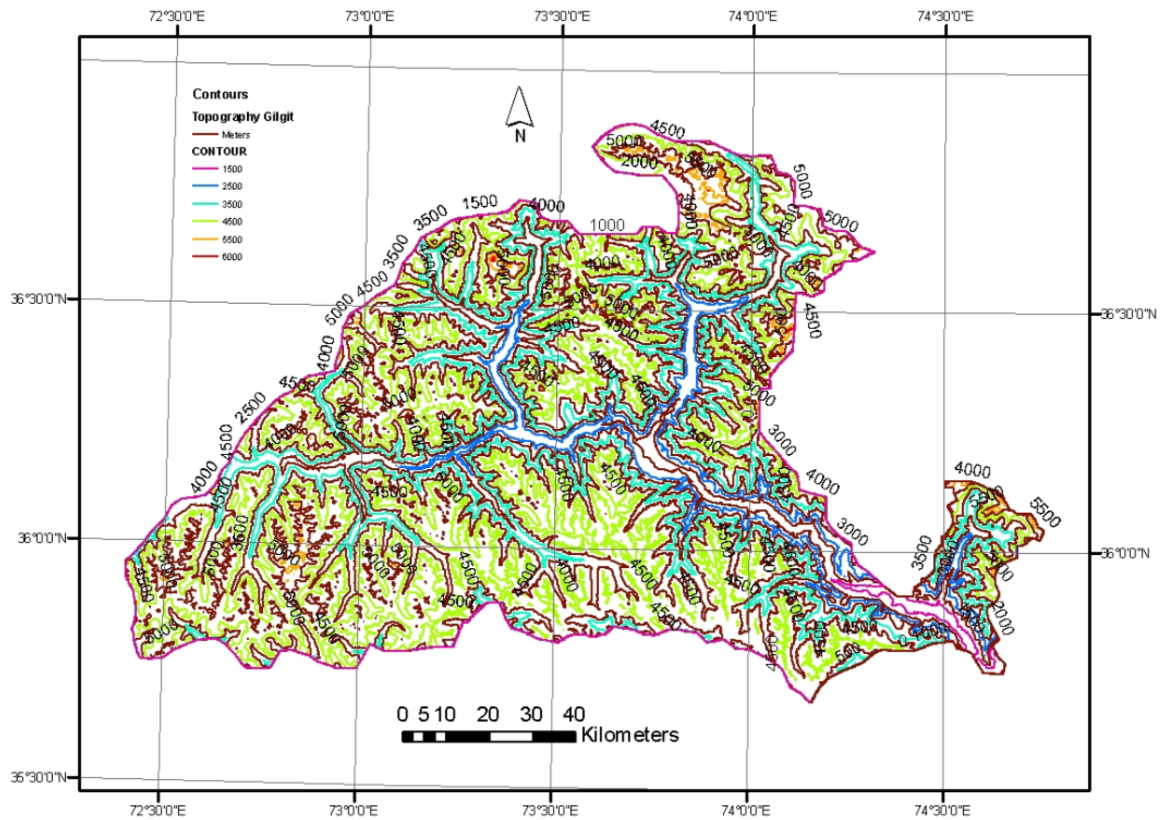

Figure 3: Topographic Map Gilgit Basin

Table 2: Division of Gilgit Basin According to Elevation Range and Area of Respective Zone

S.No	Zone Name	Elevation Range masl	Mean Hypsometric Height msal	Area (KM2)
1	A	1247-2500	2052	896
2	B	2500-3500	3091	2322
3	C	3500-4500	4083	6912
4	D	4500-5500	4782	3863
5	E	5500-6404	5660	311
Total				14304

(Figure2) shows contours delineation of zones in Gilgit Basin. Zone A ranges from 1274-2500 masl with mean hypsometric height at 2052 masl and area equals to 896 km^2. Zone B of Gilgit Basin ranges from 2500-3500 masl with mean hypsometric height as 3091masl and covers area of 2322km^2. Zone C covers spatial area of 6912km^2 i.e, largest zone with elevation range from 3500-4500 masl and mean hypsometric height as 4083 masl. Elevation ranges of Zone D is 4500-5500 masl with mean at 4782 masl and covers nearly 3863 km^2, second only to zone A. Last is zone E with least spatial coverage i.e, 311 km^2 only, and it ranges from 5500 to 6404 masl with mean at 5660 masl as expressed in Table 1. Snow cover is mapped on all elevation heights with the help of SRTM DEM as shown in Figure 2 and 3.

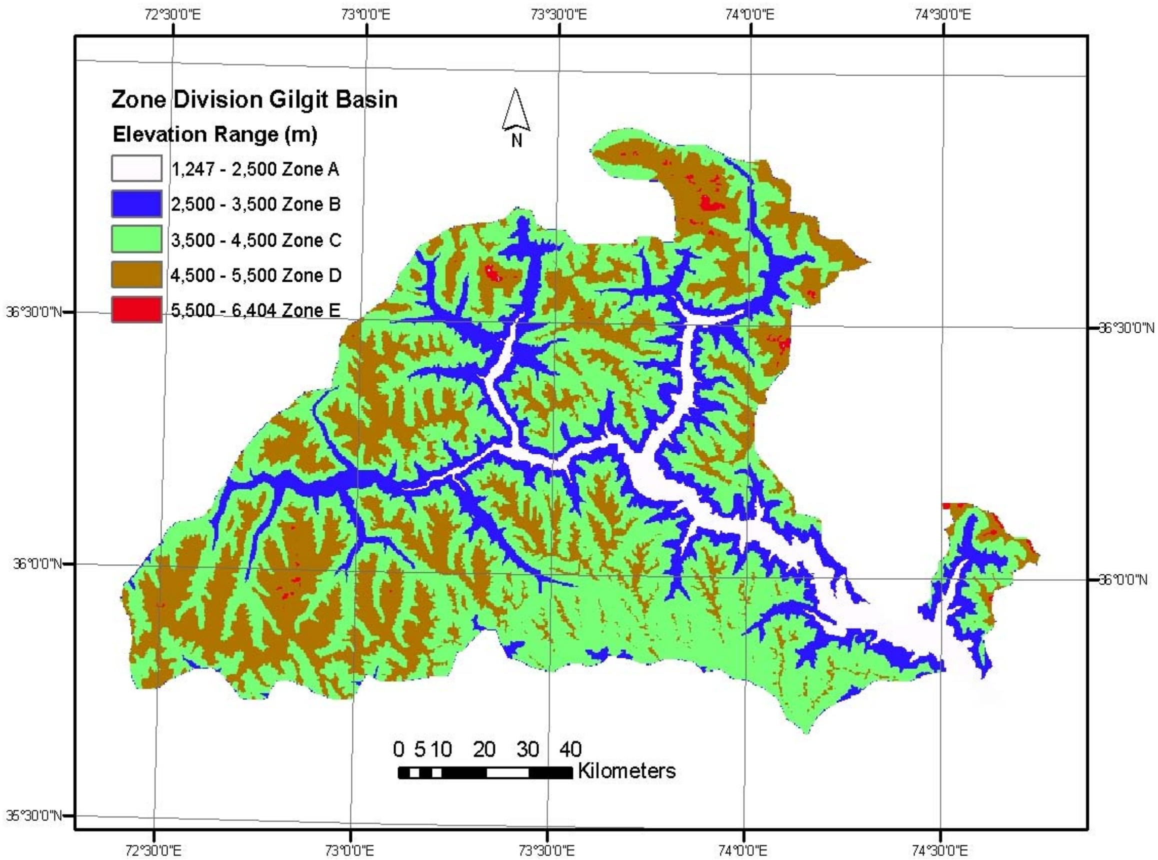

Figure 4: Zone Division SRTM DEM

Data

According to methodology that is discussed in detail below, the simulation to correlate the water produced from snowmelt and rainfalls with actual gauged discharge of the river, the following data will be used:

1) Basic data
    a. Snow Cover in square kilometer, derived through NDSI technique from MODIS data
    b. Temperature (^{o}C)
    c. Precipitation (mm)
2) Derived data
    a. Depletion Curves of snow coverage with time on all elevation ranges
    b. Runoff Coefficient
    c. Degree Day Factor
    d. Lapse Rates
    e. Recession Coefficient

Methodology

Structure of the SRM:

Each day, the water produced from snowmelt and rainfall is computed, superimposed on the calculated recession flow and transformed into daily discharge from the basin, according to Equation (1):

$$Q_{n+1} = \left[C_{sn} . a_n \left(T_n + \Delta T_n\right) S_n + C_{RN} P_n\right] \frac{\mathrm{A.10000}}{86400} \cdot \left(1\text{-}\mathrm{K}_{n+1}\right) + \mathrm{Q}_n \, \mathrm{k}_{n+1}$$

Equation 1

Where:

Q = Average Daily Discharge [m^3s^{-1}]

c = Runoff Coefficient expressing the losses as a ratio (runoff/precipitation), with C_S referring to snowmelt and C_R to rain

a = Degree-Day Factor [cm $^oC^{-1}d^{-1}$] indicating the snowmelt depth resulting from 1 degree-day

T = Number of Degree-Days [^{o}C d]

ΔT = the adjustment by temperature lapse rate when extrapolating the temperature from the station to the average hypsometric elevation of the basin or zone [^{o}C d]

S = Ratio of the snow covered area to the total area

P = Precipitation contributing to runoff [cm]. A pre-selected threshold temperature, T_{CRIT}, determines whether this contribution is rainfall and immediate. If precipitation is determined by T_{CRIT} to be new snow, it is kept on storage over the hitherto snow free area until melting conditions occur.

A = area of the basin or zone [km^2]

k = recession coefficient indicating the decline of discharge in a period without snowmelt or rainfall:

$k = \frac{Q_{m+1}}{Q_m}$ where (m, m + 1 are the sequence of days during a true recession flow period).

n = sequence of days during the discharge computation period. Equation (1) is written for a time lag between the daily temperature cycle and the resulting discharge cycle of 18 hours. In this case, the number of degree-days measured on the *n*th day corresponds to the discharge on the *n* + 1 day. Various lag times can be introduced by a subroutine.

$$\frac{10000}{86400} = \text{Conversion from cm} \cdot \text{km}^2\text{d}^{-1} \text{ to m}^3 \text{ s}^{-1}$$

T, S and P are variables to be measured or determined each day, C_R, C_S, lapse rate to determine ΔT, T_{CRIT}, k and the lag time are parameters which are characteristic for a given basin or, more generally, for a given climate.

If the elevation range of the basin exceeds 500 m, it is recommended that the basin be subdivided into elevation zones of about 500 m each. But here Gilgit Basin is divided among 5 zones (A, B, C, D, and E) each of them is nearly 1000m wide in elevation. Methodology of division is discussed below.

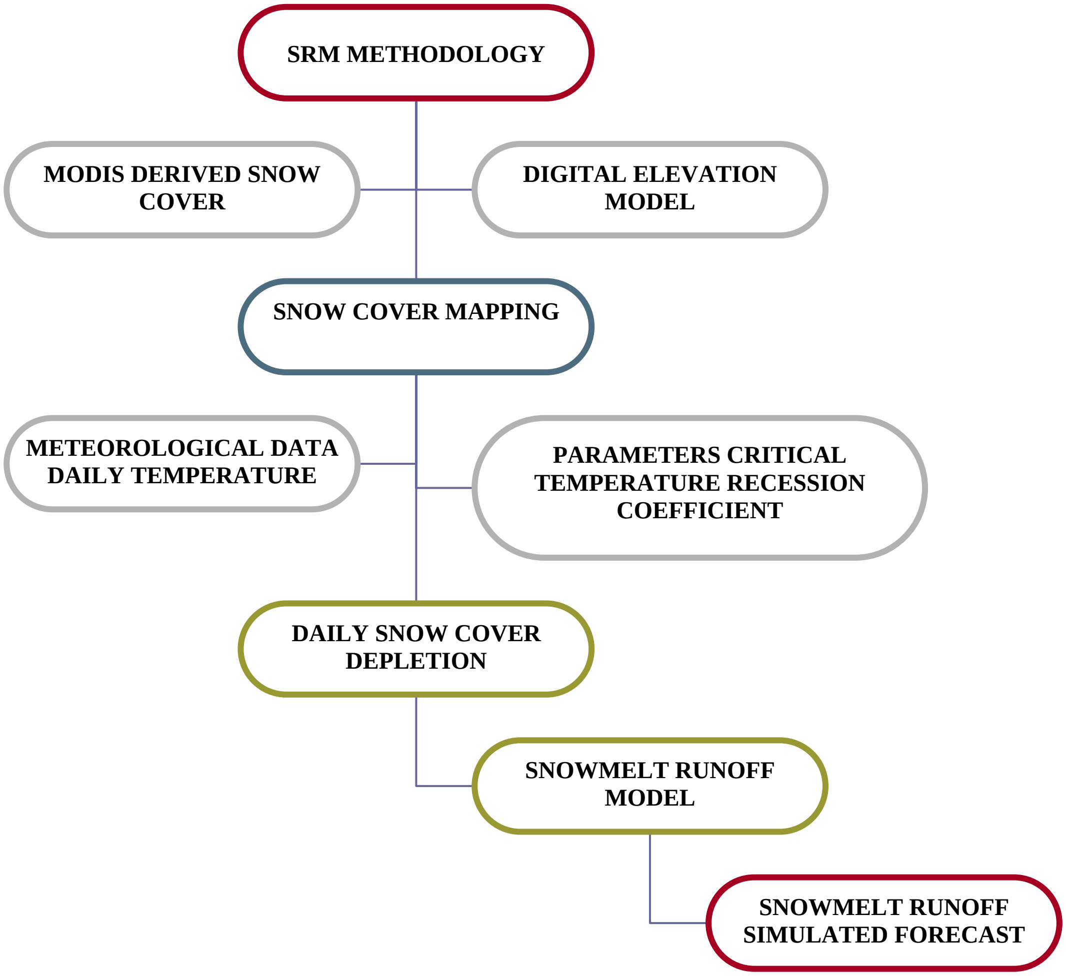

Figure 4: SRM METHODOLOGY

Satellite Snow Cover Mapping of Gilgit Basin:

To estimate the snow cover through satellite based sensor it is vital to understand the electromagnetic properties of snow. Fresh dry snow appears white to the receptors of human eye. So it is asserted as highly reflective, with little variation over the visible wavelength range (0.4-0.64 µm). Rees (2001) fully developed this argument and implied that the reflection coefficient of a snow pack should be smaller if the grain size is larger, since the number of air-ice interface and hence scattering opportunities will be reduced. Besides this, the usually increasing absorption at longer wavelength implies a commensurate reduction in reflectance at these wavelengths. Although, the density of snow does not affects reflectance directly, however, the process that causes the increase in density over time also leads to an increase in snow grain size and consequently a decrease in reflectance is observed. Furthermore, with the passage of time snow pack ages and can acquire a covering of dust or soot which may also decrease the reflectance of electromagnetic radiations (Hall and Martinec 1985).

Reflectance of the snow gets little effect by presence of the liquid water in a snow pack. The amount of water rarely exceeds 10% by volume and there is in any case competent dielectric contrast between water and ice to ensure that the multiple-scattering phenomenon continues to take place. The absorption of electromagnetic radiation in water is similar to that in ice in the visible and near-infrared regions. On the second end, the presence of liquid water does have an indirect effect on the optical properties, since it promotes clustering of the ice crystals leading to a larger effective grain size and hence lower reflectance. Model stimulations presented by (Green et al, 2001) take into account both grain size and liquid water contents as influence on the reflectance of snow. The most significant effect of increasing water content appears to be a small shift of the absorption feature at 1030nm to shorter wavelength. Reflection from a snow pack is anisotropic, with enhance specular scattering due to reflection from ice crystals (Middleton and Mungall 1952; Hall et al 1993; Knap and Reijmer 1998; Jin and Simpson 1999). However, most of the studies have neglected this effect (Konig, Winther, and Isaksson 2001).

According to Zhen and Li, (1998) Areal and spatial distribution of snow and ice cover in alpine regions vary significantly over time, due to seasonal and inter-annual variations in climate. Therefore, there is need for monitoring the Gilgit basin consisting snow-covered lofty mountains with some reliable sensor, so Moderate Resolution Imaging Spectroradiometer (MODIS) on board Terra spacecraft of Earth Observing System (EOS) of National Aeronautics and Space Administration (NASA) is selected to map Snow cover.

The capabilities of various satellites for snow cover monitoring and mapping are summarized in Table 2.

Normalized Differential Snow Index (NDSI) through MODIS:

MODIS holds special potential to address Normalized Difference Snow Index (NDSI). NDSI is prototype of Normalized Differences indices. It is originated from well known NDVI (Normalized Difference Vegetation Index). This Index artfully exploits the interaction of snow with electromagnetic radiation. Snow responses visible portion of electromagnetic spectrum with high reflectivity and in mid-infrared it reciprocates with absorption, furthermore, in same region of electromagnetic radiation (EMR) clouds are more reflective than snow (Dozier 1989). This analogy helps to discriminate snow from clouds at 1.65µm based fraction of EMR. Using this technique cirrus clouds remain troublesome to differentiate from snow (Hall *et al*, 1995). Mathematical expression of Normalized Difference Snow Index (NDSI) is as follows:

$$NDSI = \frac{(MODIS\_BAND4 - MODIS\_BAND6)}{(MODIS\_BAND4 + MODIS\_BAND6)}$$

Equation 2

Resultant pixel values exceeding 0.4 in (Equation 2) are considered as snow but it is found that this threshold limit varies with season (Vogel 2002).

An effort was made by Klein, Hall, and Riggs in 1998 and they successfully designed algorithm to map snow by using MODIS instrument. In this endeavor they defined that at pre-launch version of NDSI for MODIS, the pixels with NDSI value greater than or equal to 0.4 were considered as snow. But later on many problems were revealed in detection; two more classification criteria were introduced (Klein *et al*, 1998). “The first is an absolute reflectance in MODIS band 2 of greater than 11%. This criterion is necessary to separate snow from water, which also may have high NDSI values. The second criterion is a reflectance in MODIS band 4 of greater or equal to 10%. This prevents dark targets from being classified as snow despite high NDSI values.” All criteria are followed to map snow of Gilgit for year 2003, as expressed in (Figure 5).

Table 3: Characteristics of Satellites for Snow cover mapping

Platform Sensor	Spectral Bands	Spatial resolution	Minimum area size	Repeat period
Aircraft Orthophoto	Visible/NIR	2 m	1 km^2	flexible
IRS				
Pan	Green to NIR	5.8 m	2 km^2	24 days
LISS-II	1 – 3 Green to NIR	23 m	2.5 – 5 km^2	24 days
WiFS	1 Red / 2 NIR	188 m	10 – 20 km^2	5 days
SPOT				
HRVIR	1 – 3 Green to NIR	2.5 – 20 m	1 – 3 km^2	26 days
Landsat				
MSS	1 – 4 Green to NIR	80 m	10 – 20 km^2	16 – 18 days
TM	1 – 4 Green to NIR	30 m	2.5 – 5 km^2	16 – 18 days
ETM-Pan*	Visible to NIR	15 m	2 – 3 km^2	16 – 18 days
Terra/Aqua				
ASTER	1 – 3 Visible to NIR	15 m	2 – 3 km^2	16 days **
MODIS	1 Red / 2 NIR	250 m	20 – 50 km^2	1 day
	3 – 8 Blue to MIR	500 m	50 – 100 km^2	1 day
NOAA				
AVHRR	1 Red / 2 NIR	1.1 km	10 – 500 km^2	12 hr
Meteosat				
SEVIRI	1 – 3 Red to NIR	3 km	500 – 1000 km^2	30 min
	12 Visible	1 km	10 – 500 km^2	30 min

Acronyms:

ASTER = Advanced Spaceborne Thermal Emission and Reflection Radiometer • AVHRR = Advanced Very High Resolution Radiometer • HRVIR = High Resolution Visible and Near Infrared • IRS = Indian Remote Sensing • LISS = Linear Imaging Self-scanning Sensor • MIR = Middle Infrared • MODIS = Moderate Resolution Imaging Spectroradiometer • MSS = Multi-Spectral Scanner • NIR = Near Infrared • Pan = Panchromatic • SEVIRI = Spinning Enhanced Visible and Infrared Imager • SPOT = Satellite Pour l'Observation de La Terre • TM = Thematic Mapper • WiFS = Wide Field Sensor • ETM-Pan = Enhanced Tematic Mapper - Panchromatic

(*) Landsat 6 and 7 only (**) Depends on availability

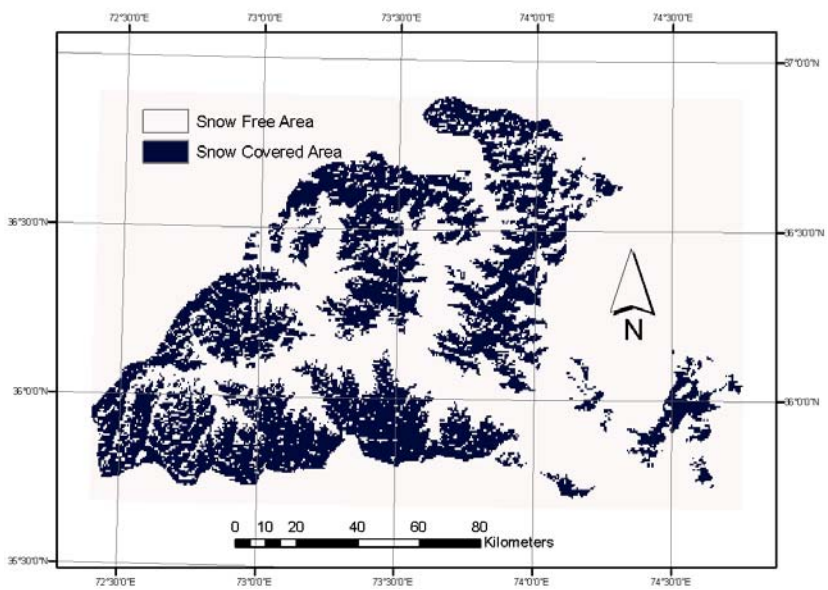

Figure 5: Snow Cover Derived through NDSI operation on Data of MODIS Terra

MODIS data is procured from NASA for year 2003 (Table 3) at regular intervals to Map snow in for Gilgit Basin.

Table 4; Image Date and Percentage of Snow cover in all Zones.

Image	Date	Zone A	Zone B	Zone C	Zone D	Zone E
2003005	05-Jan-2003	28.60335	40.55319	46.07716	49.31613	40.32258
2003021	21-Jan-03	76.26642	69.20758	68.50405	63.73285	16.72026
2003033	2-Feb-03	34.17722	34.49612	35.74942	46.54414	9.250804
2003037	6-Feb-03	100.6904	92.72179	90.07523	88.37691	19.93569
2003053	22-Feb-03	46.72037	75.1938	81.04745	93.78721	18.32797
2003065	6-Mar-03	64.44189	58.9578	56.46701	57.72716	8.038585
2003069	10-Mar-03	101.3809	98.32041	98.77025	98.93865	21.22186
2003085	26-Mar-03	57.5374	68.26012	73.81366	85.19286	19.93569
2003097	7-Apr-03	60.87457	63.65202	64.33738	75.56303	17.36334
2003101	11-Apr-03	50.51784	62.36003	69.7338	79.67901	18.00643
2003113	23-Apr-03	59.60875	55.34022	54.78877	47.06187	13.50482
2003129	9-May-03	62.14039	52.62705	53.99306	43.9037	8.038585
2003133	13-May-03	52.24396	47.20069	48.91493	62.56795	18.32797
2003149	28-May-03	91.25432	81.00775	72.25116	75.30417	16.07717
2003161	10-Jun-03	55.81128	50.68906	54.25347	42.9459	8.681672
2003165	14-Jun-03	51.78366	52.28252	45.34144	53.79239	15.11254
2003177	26-Jun-03	38.08976	37.7261	57.55208	73.59565	--
2003261	18-Oct-03	1.243094	7.92975	7.206724	8.866837	13.46154
2003277	4-Nov-03	13.80898	28.98363	30.96065	32.56536	9.646302

Depletion Curves:

Depletion curves (Figure 6) of the snow coverage is interpolated from periodical snow cover mapped trough MODIS for Gilgit Basin so that the daily values may be retrieved to be incorporated as input variable to SRM.

Snow Cover of the days in-between the images is interpolated by using linear interpolation method given as follows:

$$S_n = S_1 + \frac{S_2 - S_1}{t_2 - t_1} \times (t_n - t_1) \qquad \text{Equation 3}$$

Where S_n is Snow Cover at n^{th} day.

S1 is Snow Cover derived from first imagery.
S2 is Snow Cover derived from second imagery.
tn is number of nth day.
T1 is Julian date of first image

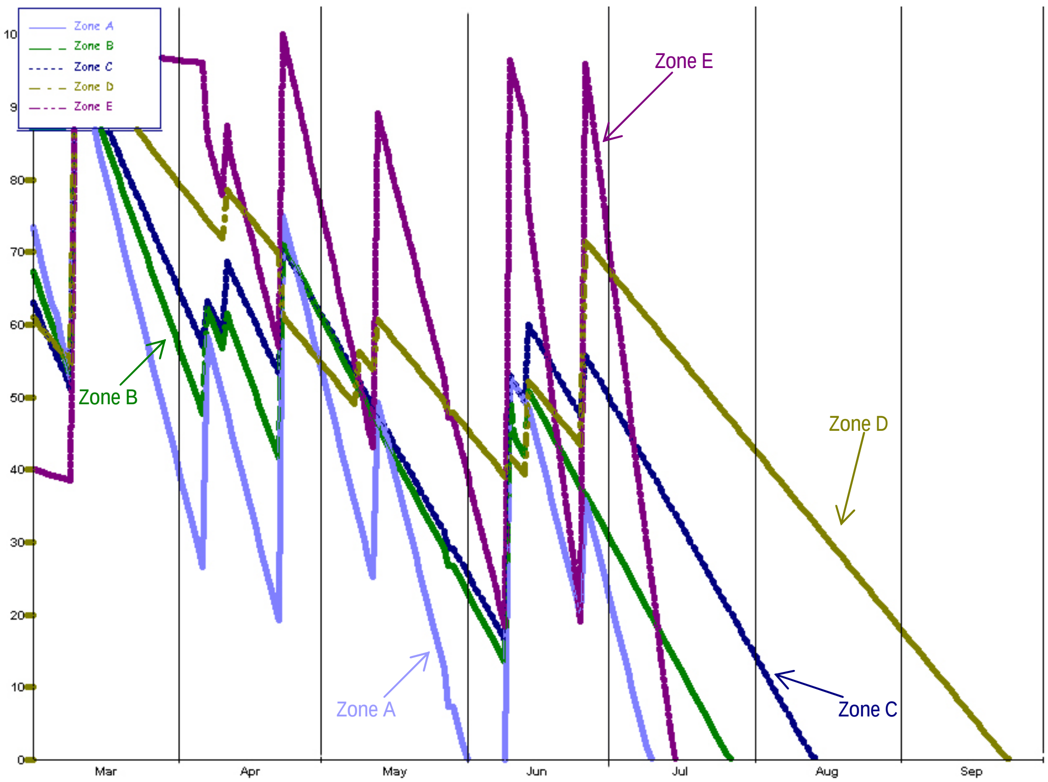

Figure 6: Snow Covered Area of all Zones of Gilgit Basin

Variables to be Incorporated in SRM:

Temperature (T):

Daily average temperature of year 2003 is utilized. The data is recorded by Pakistan Meteorological Department observatory situated at Gilgit Airport at Elevation of nearly 1460 masl.

Snowmelt Runoff Model WinSRM Version 1.10 is programmed to accept either the daily mean temperature or two temperature values on each day: T_{Max}, T_{Min}. The temperatures are extrapolated by the program from the base station elevation to the hypsometric mean elevations of the respective elevation zones (Martinec, J., Rango, A. & Roberts, R. (1992).

The model is programmed to accept either temperature data (Figure 7) from a single station or from several stations. For Gilgit observatory, the altitude of the station is entered and temperature data are extrapolated to the hypsometric mean elevations of all zones using the lapse rate.

Precipitation (P):

It is really difficult to evaluate the magnitude of rainfall of whole area in terrain like Gilgit Basin where Meteorological Observatory is situated at elevation of 1460 masl only. The Orography plays its role and magnitude of precipitation varies with respect to elevation and topography of valley.

The Snowmelt Runoff Model WinSRM Version 1.10 accepts either a single, basin-wide precipitation input or different precipitation inputs zone by zone. If the program is switched to former option and only one station happens to be available, for example Gilgit Observatory in the zone A, precipitation data entered for zone A must be copied to all other zones. Otherwise no precipitation from these zones is taken into account by the program. In basins like Gilgit Basin with a great elevation range, the precipitation input may be underestimated if only low altitude precipitation stations are available.

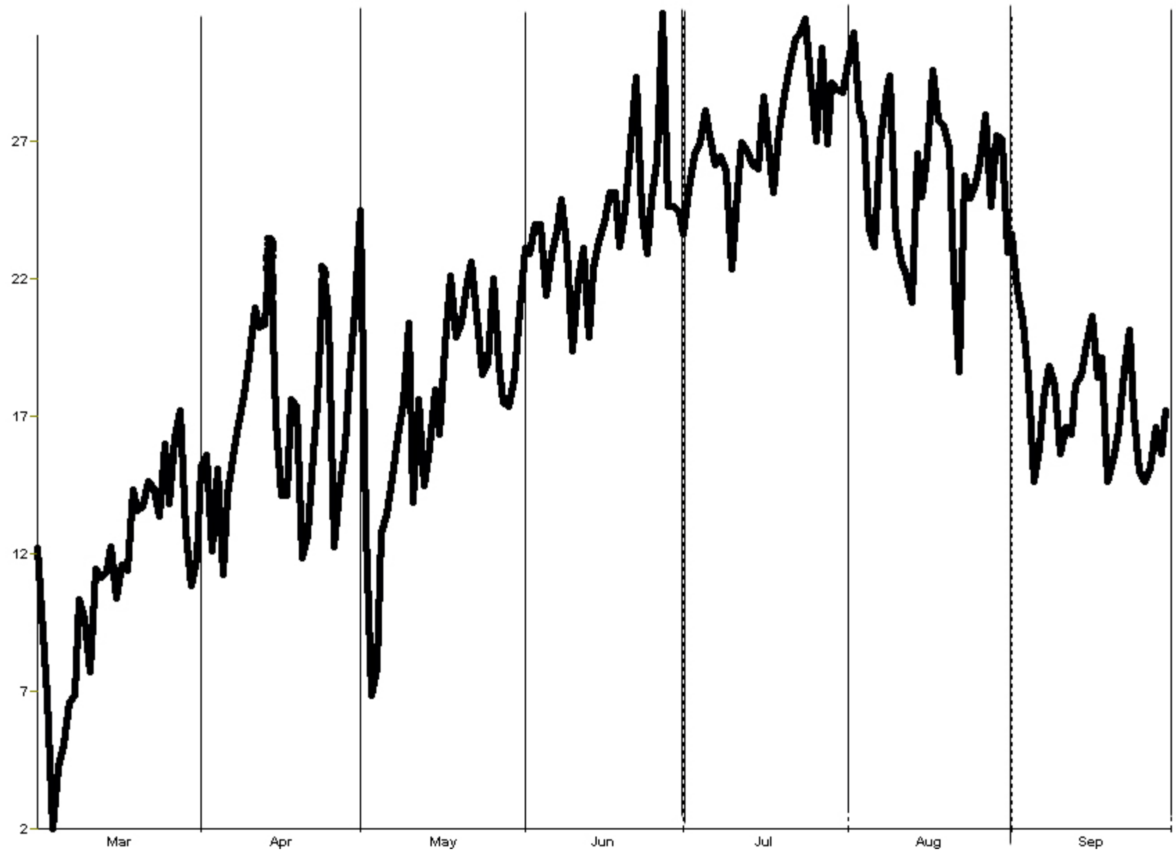

Figure 7: Average Temperature Data of Year 2003,Recorded at Gilgit Observatory

A critical temperature is used to decide whether a precipitation event will be treated as rain ($T \geq T_{CRIT}$) or as new snow ($T < T_{CRIT}$). When the precipitation event is determined to be snow, its delayed effect on runoff is treated differently depending on whether it falls over the snow-covered or snow-free portion of the basin. The new snow that falls over the previously snow-covered area is assumed to become part of the seasonal snowpack and its effect is included in the normal depletion curve of the snow coverage. The new snow falling over the snow-free area is considered as precipitation to be added to snowmelt, with this effect delayed until the next day warm enough to produce melting.

(Figure 8) is graphical depiction of incorporated precipitation of Gilgit Basin recorded at 1460 masl elevation.

Runoff coefficient (c):

This coefficient is referred to the losses (Martinec, J., Rango, A. & Roberts, R. (1992) , i.e., difference between the available water volume (Liquid and solid precipitation) and the outflow from the basin. It corresponds to the ratio of the measured precipitation to the measured runoff. Runoff coefficient values are obtained by comparing historical precipitation and runoff ratios for a long time. However, these ratios are difficultly obtained in view of the precipitation gauge catch deficit which particularly affects snowfall and of inadequate precipitation data from rigorous mountain regions. At the start of the snowmelt season, losses are usually very small as they are confined to evaporation from the snow surface, especially at high elevations. In the letter stage, with the exposure of soil and growth of vegetation, more losses are expected due to evapotranspiration and interception. Towards the end of the snowmelt season, direct channel flow from the remaining snowfields and glaciers may prevail in some basins which lead to a decrease of losses and to an increase of the runoff coefficient. In addition, c is usually different for snowmelt and for rainfall.

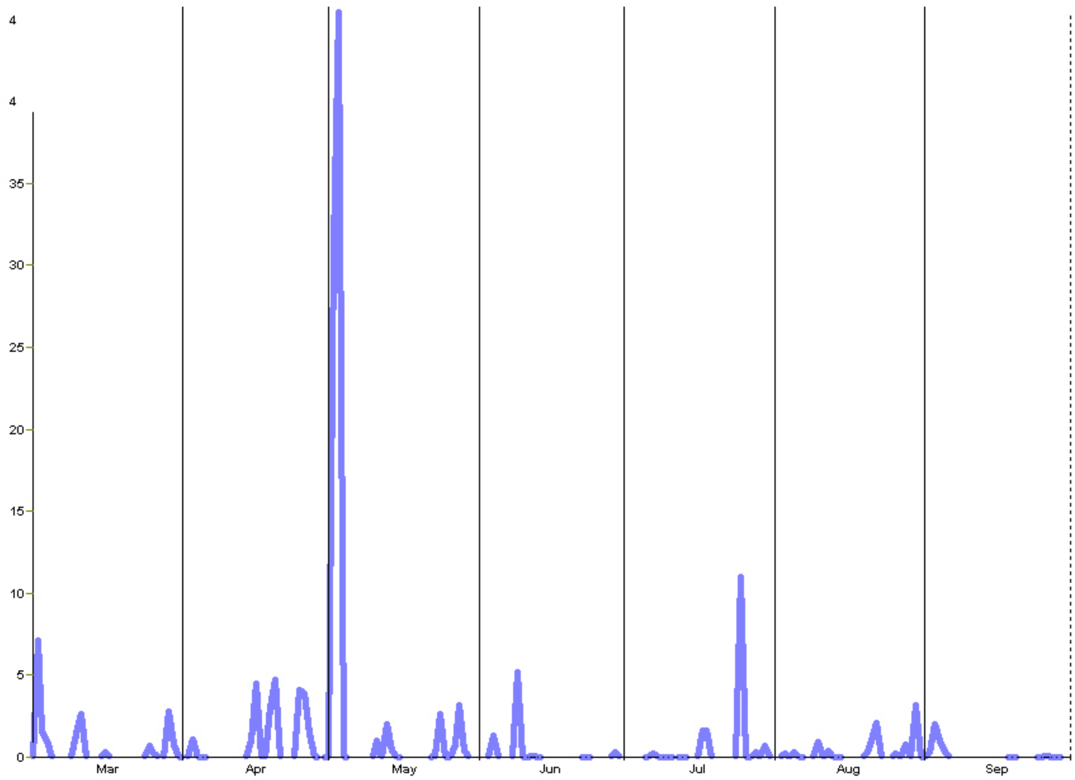

Figure 8: Precipitation March- September 2003

Of the SRM parameters, the runoff coefficient appears to be the primary candidate for adjustment if a runoff simulation is not at once successful. (Martinec, J., Rango, A. & Roberts, R. (1992)

Degree-day factor (a):

The degree-day factor a [$cm^{o}C^{-1}d^{-1}$] converts the number of degree-days T [$^{o}C \cdot d$] into the daily snowmelt depth M [cm]:

$$M = a \cdot T \qquad \text{Equation 4}$$

Another approach to evaluate Degree Day is comparing Degree-Day values with the daily decrease of the snow water equivalent which is measured by radioactive snow gauge, snow pillow or a snow lysimeter. Such measurements (Martinec, 1960) have shown a considerable variability of degree-day ratios from day to day. This is understandable because the degree-day method does not take specifically into account other components of the energy balance, notably the solar radiation, wind speed and the latent heat of condensation.

For terrain like Gilgit basin where topography experience various types of meteorological conditions according to elevation, aspect and landforms, one value of Degree Day Factor can not be considered justified for all sort of conditions in a zone. This is limitation of SRM model. Furthermore, the degree-day factor is not a constant. It changes according to the changing snow properties during the snowmelt season.

During PMD expedition to Hinarchi Glacier, Bagrot Valley, Gilgit, in 2008 Degree Day Factor was measured for different type of glaciated ice and snow, which includes debris covered glacier, firn, bare ice cliffs and snow bestowed by summer snowfalls. These values range from 0.001 up to 0.6 $cm^{o}C^{-1}d^{-1}$.

In this strive SRM is simulated at different, nearly real time degree-day factor values to yield best possible results.

Temperature Lapse Rate (γ):

A true picture of lapse rate is made by using Automatic Weather Station (AWS) data placed at Askole and Urdukas at Baltoro Glacier. Details of lapse rate derived through monthly averages are discussed in Table 4.

Table 5: Average Lapse Rate for Gilgit Basin

Month	Average Lapse Rate ^{o}C/ 100 m
January	0.656
February	0.645
March	0.738
April	0.767
May	0.814
June	0.768
July	0.711
August	0.733
September	0.651
October	0.902
November	0.864
December	0.774

Recession Coefficient (k):

As already discussed recession coefficient indicating the decline of discharge in a period without snowmelt or rainfall:

$$k = \frac{Q_{m+1}}{Q_m} \qquad \text{Equation 5}$$

Where (m, m + 1 are the sequence of days during a true recession flow period).

Recession coefficient is derived through measured runoff. Its value varied with the season. For instance its value is above 1 for season attributed with increase of snowmelt runoff, where as in months of August and September it remarkably decreased.

Results:

Seasonal Snow Cover for Gilgit basin for year 2003 is estimated using MODIS data and NDSI technique. Gaps between the snow cover data is filled through linear interpolation method. Meteorological data based on average temperature and precipitation of the melt season of year 2003 is incorporated. Runoff measured by WAPDA at Alam Bridge for Gilgit Basin for year 2003 is used for comparison and calibrations. Parameters like runoff coefficient, degree day factor, temperature lapse rate and recession coefficient, either derived from field and evaluated from raw date or from historical record is provided for SRM Version 1.10.

SRM holds very promising results for the Gilgit Basin. Minor adjustments in Recession Coefficients and Degree Day Factor brought very articulate results. Volume difference between Measured Runoff and Computed Runoff varied from 1.62% to 29.73%, which is acceptable. Graphical comparison of measured and computed runoff is presented in (Figure 8).

SRM with MODIS derived Snow Cover and articulate DEM is very effective to estimate seasonal snowmelt runoff. Once parameterized it is also efficient to forecast un-gauged basins.

(Table 5) defines the comparison, between Measured and Computed Runoff Volumes and, between Average Measured and Computed Runoff along with volume different (%). (Figure 9) is graphical depiction of Runoff (measured vs computed) for September 2003.

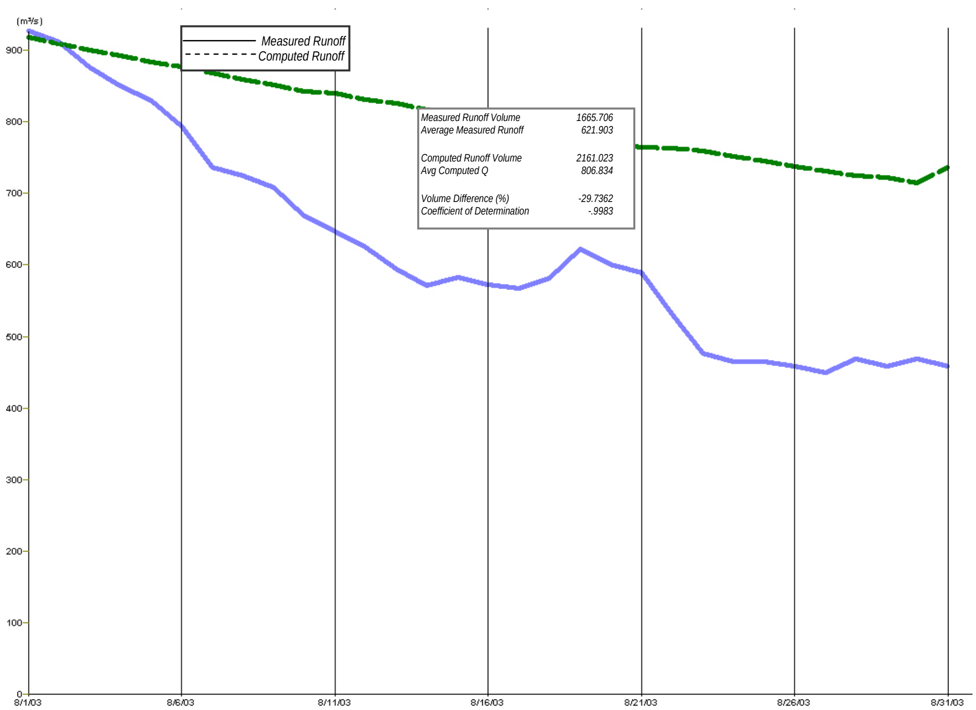

Figure 9: Runoff (Measured vs. Computed) for August 2003.

Table 6: Comparison of Measured and Computed Runoff Volumes and Averages Runoff

Month	**Measured Runoff Volume ($10^6 m^3$)**	**Average Measured Runoff (m^3/s)**	**Computed Runoff Volume ($10^6 m^3$)**	**Average Computed Runoff (m^3/s)**	**Volume Difference (%)**
March 2003	133.4	49.806	138.755	51.805	-4.01
April 2003	181.44	70	162.73	62.78	10.31
May 2003	616.46	230.161	639.37	238.71	-3.71
June 2003	2666.82	1028.86	2710.09	1045.56	-1.62
July 2003	3163.27	1181.03	3253.06	1214.5	-2.83
August 2003	1665	621	2161	806	-29.73
September 2003	1024.79	395.36	1048.681	404.504	-2.321

Conclusions, Limitations and Recommendations

It is really difficult to evaluate the magnitude of rainfall of whole area in terrain like Gilgit Basin where Meteorological Observatory is situated at elevation of 1460 masl only. The Orography plays its role and magnitude of precipitation varies with respect to elevation and topography of valley and in basins like Gilgit Basin with a great elevation range, the precipitation input may be underestimated if only low altitude precipitation stations are available.

Furthermore, the correlation between measured and computed runoff offered exaggerated values because of insufficient data of precipitation for basin.

Similarly in case of Runoff Coefficient, as it corresponds to the ratio of the measured precipitation to the measured runoff, and Runoff coefficient values are obtained by comparing historical precipitation and runoff ratios for a long time. These ratios are difficultly obtained in view of the precipitation gauge catch deficit, which particularly affects snowfall and of inadequate precipitation data from rigorous mountain regions.

Among the SRM parameters, the runoff coefficient appears to be the primary candidate for adjustment if a runoff simulation is not at once successful.

Another issue is Degree Day Factor, for terrain like Gilgit basin where topography experience various types of meteorological conditions according to elevation, aspect and landforms, one value of Degree Day Factor cannot be considered justified for all sort of conditions in a zone. This is limitation of SRM model. Furthermore, the degree-day factor is not a constant. It changes according to the changing snow properties during the snowmelt season.

In purview of above mentioned limitations, it is suggested that a number of AWS must be installed at various locales and different altitudes to draw an effective picture of temperature and precipitation. As in present study only one station observations are used, that led many parameters to be estimated hypothetically.

Similarly, it is need to measure snow depth at multiple points in study area with some articulated method to design an in-depth understanding of behaviour of Degree Day Factor.

In the last, it is needed to imitate this study for same and other basin for numbers of years to sketch a good picture of inputs and resultant outputs, so this approach can be used for forecasting runoff during melting season in Northern Pakistan.

References:

Anderson, E.A (1976). National river forecast system-snow accumulation and ablation model, NOAA Tech. Memo. NWS Hydro-17, US Dept of Commerce, Silver Spring, USA.

Green, R. O., J. Dozier, D. Roberts, and T. Painter. 2002. Spectral snow-reflectance models for grain size and liquid water fraction in melting snow for the solar reflected spectrum. *Annals of Glaciology* 32:71-73.

Hall, D.K., and J. Martinec. 1985. *Remote Sensing of Ice and Snow*. London: Chapman and Hall.

Jin, Z., and J.J Simpson. 1999. Bidirectional anisotropic reflection of snow and sea in AVHRR channel 1 and 2 spectral regions—Part1: theoretical analysis. *IEEE Transaction on geosciences and Remote Sensing 37*9(1): 543-554

Klein, A. G., Hall, D. K., & Riggs, G. A. (1998). Global snow cover monitoring using MODIS. In Proceedings of the 27th International Symposium on Remote Sensing of the Environment, 8-12 June 1998, Tromso, Norway. ISRSE.

Knap, W.H., and C.H. Rejimer. 1998. Anisotropy of the reflected eradiation field over malting glacier ice: Measurements in Landsat TM Bands2 and 4. *Remote Sensing of Environemnt65:93-104.*

Konig, M., J-G. Winther, and E. Isaksson. 2001. Measuring snow and glacier ice properties from satellite. *Reviews of Geophysics* 39 (1):1-27.

Martinec, J. (1975) Snowmelt-Runoff Model for stream flow forecasts. Nordic Hydrol. 6(3), 145-154.

Martinec, J., Rango, A. & Roberts, R. (1992), The Snowmelt-Runoff Model (SRM) User’s Manual, Edition 2005, USDA Jornada Experimental Range, New Mexico State University, Las Cruces, NM, U.S.A.

Martinec, J., Rango, A. and Roberts R. (1994). The Snowmelt-Runoff Model (SRM) User's Manual (Ed.: M.F. Baumgartner). Geographica Bemesia, Department of Geography, University of Bern, Bern, Switzerland, 29p.) (Rango, A. and Martinec, J. (1995). Revisiting the degree-day method for snowmelt computation.

Middleton, W.E., and A.G. Mungall. 1952. The luminous directional reflectance of snow. *Journal of the Optical Society of America* 42:572-579.) (Hall, D.K., J.L. Foster, J.R. Irons, and P.W. Dabney. 1993. Airborne bidirectional radiances of snow-cover surface in Montana, USA. Annals of Glaciology 17:35-40.

Quick, M.C. and Pipes, A. (1988). High mountain snowmelt and application to runoff forecasting, Proc. of Workshop on Snow Hydrology, held at Manali from Nov. 23-26, 1988, pp IV1-32.

Rees, W Gareth., Published 2006., REMOTE SENSING OF SNOW AND ICE. Taylor & Francis Group.

Singh P., Jain, S. K. and Naresh Kumar (1997). Estimation of snow and glacier-melt contributing to the Chenab river, Western Himalaya, Mountain Research and Development, 17(1):49- 56.

Zhen, X., and Li, J., 1998, Remote Sensing monitoring of glaciers, snow and lake ice in Qinghai-Xizang (Tibetan) Plateau and their Influence on Environments, edited by M. Tang, G. Cheng and Z. Lin (Guangzhou, China: Guandong Sciences and Technology Press) pp.279-308.

Vogal, S.W. 2002. Usage of high-resolution Landsat 7 and 8 for single-band snow-cover classification. *Anneal of Glaciology*, vol.34, pp.53-57.